Published OnlineFirst May 11, 2010; DOI: 10.1158/1078-0432.CCR-09-3199

Cancer Therapy: Preclinical

Clinical Cancer Research

Efficacy, Biodistribution, and Pharmacokinetics of CD22-Targeted Pegylated Liposomal Doxorubicin in a B-cell Non–Hodgkin's Lymphoma Xenograft Mouse Model

Joseph M. Tuscano[1,2], Shiloh M. Martin[1], Yunpeng Ma[1], William Zamboni[3,4,5,6], and Robert T. O'Donnell[1,2]

Abstract

Purpose: Non–Hodgkin's lymphoma (NHL) is the sixth most common cause of cancer death in the U.S. Pegylated liposomal doxorubicin (PLD) is a liposomal form of doxorubicin (DXR) that causes less toxicity than does free DXR. To further enhance efficacy and decrease toxicity, we conjugated HB22.7, an anti-CD22 monoclonal antibody to PLD, thus creating CD22-targeted immunoliposomal PLD (IL-PLD).

Experimental Design: *In vitro* cytotoxicity of IL-PLD and PLD was assessed in CD22-positive and CD22-negative cell lines. Biodistribution, myelotoxicity, and plasma pharmacokinetics were measured in NHL xenograft–bearing mice treated with IL-PLD or PLD. Survival, tumor volume, and toxicity (WBC counts, body weights) were assessed in mice receiving a single dose (8, 12, or 16 mg DXR/kg) or three doses (8 mg DXR/kg/dose) of IL-PLD; controls were PLD, free DXR, PLD plus unconjugated HB22.7, IL-null (HB22.7-conjugated empty liposome), and nontreated mice.

Results: IL-PLD improved cytotoxicity over PLD only in CD22-positive cells. IL-PLD displayed similar pharmacokinetics and toxicities as PLD. Tumor DXR accumulation was greater and tumor/normal tissue ratios were similar (spleen) or greater (kidney, lung, and liver) in mice treated with IL-PLD versus PLD. IL-PLD reduced tumor volume more effectively than PLD at all doses; the three-dose regimen was superior. The three-dose regimen was used in confirmatory studies, which showed that IL-PLD produced significantly greater tumor volume reduction and enhanced survival versus PLD.

Conclusion: IL-PLD has increased efficacy without increased toxicity compared with PLD. This suggests that IL-PLD may be an improved form of DXR-based therapy of NHL. *Clin Cancer Res; 16(10); 2760–8.* ©*2010 AACR.*

Non–Hodgkin's lymphoma (NHL) is the sixth most common cause of cancer-related deaths in the United States and the incidence has nearly doubled since the 1970s (1). Most NHL are initially responsive to chemotherapy; however, the efficacy of chemotherapy is often limited by toxicity and relapse is common (2).

Doxorubicin (DXR) is one of the more effective chemotherapeutic agents that are commonly used to treat NHL. DXR is an anthracycline antibiotic that intercalates into the DNA of rapidly dividing cells, thereby inhibiting nucleic acid synthesis (3). Dose-limiting toxicities of DXR include cardiomyopathy (4) and myelosuppression (5, 6); alopecia, nausea, vomiting, and stomatitis are also common (5). When compared with free (nonliposomal) DXR, liposomal formulations of DXR [such as pegylated liposomal doxorubicin (PLD)] have reduced toxicity, prolonged exposure in blood and tissue (area under the time versus concentration curve; ref. 7), and increased accumulation of DXR in solid tumors (8). The increased accumulation of DXR in tumor and the decreased toxicity of PLD result from the ability of liposomes to extravasate through fenestrated tumor vessels, whereas in normal tissues, liposomes tend to remain confined to the intravascular space (9, 10). Conjugating monoclonal antibodies (mAb) to liposome-containing drugs (thereby creating immunoliposomes) can further reduce toxicity and increase efficacy by targeting the drug specifically to the tumor. PLD has been successfully targeted to tumors using anti-CD19 mAbs (11, 12).

NHLs are a heterogeneous group of lymphoid malignancies, ~90% of which are of B-lymphocyte origin (2). CD22 is a B lymphocyte–specific glycoprotein expressed

Authors' Affiliations: [1]Division of Hematology and Oncology, Department of Internal Medicine, University of California, Davis, [2]Northern California Veteran's Administration Healthcare System, [3]Division of Pharmacotherapy and Experimental Therapeutics, UNC Eshelman School of Pharmacy, [4]Molecular Therapeutics Program, UNC Lineberger Comprehensive Cancer Center, [5]UNC Institute for Pharmacogenomics and Individualized Therapy, [6]Carolina Center of Cancer Nanotechnology Excellence, University of North Carolina, Chapel Hill, North Carolina

Corresponding Author: Joseph Tuscano, UC Davis Cancer Center, Division of Hematology and Oncology, 4501 X Street, Suite 3016, Sacramento, CA. 95817. Phone: 916-734-3771; Fax: 916-734-2361; E-mail: joseph.tuscano@ucdmc.ucdavis.edu.

doi: 10.1158/1078-0432.CCR-09-3199

Published OnlineFirst May 11, 2010; DOI: 10.1158/1078-0432.CCR-09-3199

Translational Relevance

Although current therapy for Non–Hodgkin's lymphoma (NHL) produces high response rates, the majority of patients cannot be cured. CD22 is a B lymphocyte–specific phospho-glycoprotein that is present on most NHL. Our studies have dissected the CD22 signaling cascade at the biochemical level. We identified unique anti-CD22 monoclonal antibodies that specifically block the interaction of CD22 with its ligand, effectively cross-link CD22, have *distinct* functional properties that mediate apoptosis, and have substantial *in vivo* lymphomacidal activity. The monoclonal antibody HB22.7, when bound to CD22, mediates internalization, and thus, in the present study, HB22.7 is being used as a vehicle for intracellular drug delivery. Doxorubicin is one the most effective chemotherapeutic agents for NHL therapy, but its efficacy is limited by toxicity. Based on the known efficacy of doxorubicin and the independent lymphomacidal activity of HB22.7, the use of HB22.7 as vehicle to specifically deliver pegylated liposomal doxorubicin to NHL was studied.

by nearly all mature B lymphocytes, but not on pre-B cells or terminally differentiated plasma cells. Besides its function as a cell adhesion molecule and as a sialic acid-binding lectin, CD22 also modulates signal transduction through the B-cell receptor. Although the ligand for CD22 remains largely unknown, upon ligation with anti-CD22 mAbs, CD22 is internalized (13–15). The anti-CD22 mAb, HB22.7, binds the two NH_2-terminal immunoglobulin domains and blocks CD22 ligand binding. Specifically blocking the interaction of CD22 with its ligand effectively induces proliferative responses in primary B cells but induces apoptotic responses in neoplastic B cells (16). In contrast, other anti-CD22 mAbs that do not block ligand binding have only modest functional effects (16, 17). In addition, a recent report that used animals lacking the CD22 ligand binding domains and used mouse anti-mouse anti-CD22 mAbs confirmed the requirement of CD22 ligand blocking for malignant B-cell elimination (18). Previous studies using HB22.7 have shown significant preclinical efficacy in human NHL xenograft models (16) and HB22.7 has been humanized and is awaiting human clinical trials. Because most NHL express CD22 that becomes internalized upon ligation, CD22 is a promising target for toxin or radioisotopemediated immunotherapy.

We previously reported the initial *in vitro* characterization of CD22-targeted immunoliposomal PLD (IL-PLD; ref. 19) and the lymphomacidal properties of HB22.7 in nude mice bearing Raji (human B-cell NHL) xenografts (16). Using the same xenograft model in this study, we assessed the preclinical efficacy, biodistribution, and plasma pharmacokinetics in mice treated with CD22-targeted IL-PLD.

Materials and Methods

Reagents and antibodies. Hydrogenated soy phosphatidylcholine, maleimide-derivatized polyethylene glycol (PEG2000)-distearoylphosphotidylethanolamine (Mal-PEG-DSPE), methoxy-polyethylene glycol-DSPE (mPEG2000-DSPE), and cholesterol were purchased from Avanti Polar Lipids. Sephadex G-50, Sepharose CL-4B, HEPES, reduced Triton X-100, and 2-iminothiolane (Traut's reagent) were purchased from Sigma Co. PLD; stericly stabilized liposomes containing entrapped DXR was manufactured by Ortho Biotech Products, LP. Goat anti-mouse immunoglobulins fluorescein conjugate (goat anti-mouse Ig-FITC) was purchased from Biosource. BCA protein assay kit and Silver SNAP II Stain kit were purchased from Pierce. RPMI 1640, penicillin-streptomycin, and fetal bovine serum were purchased from Life Technologies. The anti-CD22 mAb, HB22.7, was purified from ascites and has been previously characterized (15). All chemicals were of analytic grade purity.

Cell lines. The CD22-positive human Burkitt's B-cell lymphoma line, Raji (ATCC CCL-86), CD22-positive human Burkitt's B-cell lymphoma line, Ramos (ATCC CRL-1596), and CD22-negative human T-cell leukemia line, Jurkat (ATCC TIB-152) were all purchased from the American Type Culture Collection. All cells were thawed and grown in suspension in complete RPMI 1640 (supplemented with 10% fetal bovine serum, 50 U/mL penicillin G, and 50 μg/mL streptomycin sulfate) and maintained in tissue culture flasks at 37°C in 5% CO_2 and 90% humidity. After two passages, multiple vials were refrozen and stored in liquid nitrogen for future use. Fresh vials of cells are periodically thawed and used for *in vitro* experiments to ensure that changes to cells have not occurred over time/passages in culture. For all xenograft studies, a fresh vial of Raji cells is thawed 7 to 10 days before tumor cell implantation.

Preparation of liposomes. Empty (null) liposomes (containing no DXR) were composed of hydrogenated soy phosphatidylcholine/cholesterol/mPEG2000 at a molar ratio equivalent to that of PLD. Lipids were dried from chloroform with nitrogen gas for 15 minutes to make a thin film covering the inside of a glass tube and dried further in a speed vacuum for 4 to 6 hours. Lipids were then hydrated in 25 mmol/L HEPES saline buffer (pH 7.4) by warming in a 65°C water bath and stirring for 1 hour. Liposomes were then sonicated at 4°C until clear. PLD, a long-circulating liposomal formulation of DXR, was prepared and characterized at ALZA Corp. as previously described (20).

The anti-CD22 mAb, HB22.7, was conjugated to PLD or empty liposomes using a previously described postinsertion method for transfer of ligands to preformed liposomes (21). Briefly, Mal-PEG-DSPE and mPEG-DSPE were mixed at a 4:1 molar ratio and dried under nitrogen gas until no liquid remained. The lipid mixture was further dried in a

Published OnlineFirst May 11, 2010; DOI: 10.1158/1078-0432.CCR-09-3199

speed vacuum for an additional 4 hours. The dried lipid films were hydrated in deoxygenated 25 mmol/L HEPES (pH 7.4) to a concentration of 10 mmol/L by heating in a 65°C water bath immediately before mAb coupling. HB22.7 (10 mg/mL) was incubated with 2-iminothiolane in O_2-free HEPES-buffered saline (pH 8.0) at a molar ratio of 10:1 for 1 hour at room temperature to thiolate the NH_2 groups of the mAb. The thiolated mAb was then chromatographed over a Sephadex G-50 column equilibrated with O_2-free HEPES-buffered saline (pH 7.4) and immediately incubated with hydrated micelles overnight under nitrogen gas with continuous stirring. After mAb coupling to micelles, the micelles were incubated with preformed liposomes (PLD or empty liposomes) at a molar ratio of 0.05:1 for 1 hour at 60°C. The micelle/liposome mixture was then chromatographed over a Sepharose CL-4B column equilibrated in pyrogen-free HEPES-buffered saline (pH7.4) to separate the immunoliposomes (IL-PLD or IL-null) from PEGmicelles and free mAb. The amount of mAb conjugated to the liposomes was quantified using a BCA protein assay kit and the coupling ratio (μg IgG/μmol liposome phospholipid) was calculated. Phospholipid concentration was determined by the Fiske and Subbarow method (22) and verified by SDS-PAGE. The concentration of the liposome-entrapped DXR was determined by spectrophotometry (λ = 490 nm) and compared with a reference standard curve. The size of the resulting IL-PLD was determined by dynamic light scattering using a Beckman Coulter N4 MD submicron particle analyzer.

Mice. Six- to 8-week-old female BALB/c nude mice were obtained from Harlan Sprague-Dawley and maintained in microisolation cages under pathogen-free conditions in the UC Davis animal facility.

In vitro *cytotoxicity assays.* Raji, Ramos, or Jurkat cells ($2\text{-}2.5 \times 10^4$) were plated in 96-well round-bottomed plates in a volume of 100 μL per well. PLD or IL-PLD was serially diluted with medium to achieve final DXR concentrations of 0.04 to 2.5 μg/mL. Control cells received medium only. All samples were plated in triplicate. The plates were incubated at 37°C in 5% CO_2 and 90% humidity for 72 hours. Cell viability was assessed by trypan blue exclusion assay.

DXR accumulation in blood cells, tissues, and NHL xenografts after IL-PLD or PLD treatment. Mice received whole body irradiation (400 rads). Three days after irradiation, 0.5×10^7 Raji cells were implanted s.c. on the left flank. Twenty-one days after implantation, mice were treated i.v. through the tail vein, with either IL-PLD or PLD at a dosage of 10 mg DXR/kg (n = 8 mice per treatment). Immediately after treatment, mice were subdivided into two groups, one for blood pharmacokinetics (n = 4 mice per treatment) and one for biodistribution (n = 4 mice per treatment). For blood pharmacokinetics, 10 μL of blood were collected (through tail vein nicking) from each mouse at 0.17, 0.5, 1, 2, 4, 8, 24, 48, and 72 hours after treatment. Blood was immediately diluted into 250 μL of 0.5 mmol/L EDTA-PBS, followed by a 5-minute centrifugation at 300 × g. Plasma was collected and DXR was extracted from plasma by acidified isopropanol (75mmol/L hydrochloric acid in 90% isopropanol) for 20 hours at 4°C. The sum total (encapsulated and released) DXR was assayed using a microflourometer, using 470 nm as the excitation and 590 nm as the emission wavelength. For biodistribution, mice were euthanized 24 hours after treatment and tumor, liver, spleen, kidneys, and lungs were removed, washed, weighed, and single-cell suspensions were made. DXR was extracted from cells by acidified isopropanol (75 mmol/L hydrochloric acid in 90% isopropanol) for 20 hours at 4°C. The sum total (encapsulated and released) DXR was assayed as described above. For pharmacokinetics, DXR concentration is expressed as microgram per liter of blood plasma. For biodistribution, DXR concentration is expressed as nanogram per gram of tissue. Tumor/normal tissue (T/NT) ratios were calculated for each organ by dividing tumor DXR concentration by DXR concentration of each organ.

NHL xenograft animal studies. Mice were irradiated and 0.5×10^7 Raji cells were implanted as described above. For the first study, 1 day after tumor implantation, mice were randomly divided into nine groups (n = 8 per group). Six of the groups were administered a single dose of either PLD or IL-PLD at doses of 8, 12, or 16 mg DXR/kg on day 1 after implantation. Two groups received three doses of either PLD or IL-PLD at doses of 8 mg DXR/kg/dose on days 1, 8, and 15 after implantation. The ninth group was treated with three doses of PBS at the same volume as PLD or IL-PLD. All treatments were administered through the tail vein.

For the second xenograft study, 1 day after implantation, mice were randomly assigned to five different treatment groups (n = 8 mice per group). All treatments were administered through the tail vein on days 1, 8, and 15 after tumor implantation. For the first group, IL-PLD was administered at 8.0 mg DXR/kg/dose. At this dose of IL-PLD, the corresponding lipid and HB22.7 mAb doses were 0.8 to 1 μmol of phospholipids and 200 μg HB22.7 per dose. For the second group, PLD was administered at 8.0 mg DXR/kg/dose. For the third group, PLD plus free HB22.7 were administered at 8.0 mg DXR/kg/dose plus 200 μg/dose of unconjugated HB22.7. For the fourth group, IL-null (HB22.7-conjugated empty liposomes containing no DXR) was administered at 1 μmol phospholipid and 200 μg of HB22.7 per dose. For the fifth group, PBS was administered at the same volume as IL-PLD.

For both xenograft studies, tumors were measured twice per week by caliper and tumor volumes were calculated using the equation (length × width × depth) × 0.52. Mice were euthanized when the tumor reached 20 mm in any dimension.

Statistics for xenograft studies. Tumor volume data were analyzed using Kaplan-Meier curves. For this analysis, an "event" was defined as tumor volume reaching 450 mm^3 or greater. Each individual mouse was ranked as a 1 (event occurred) or a 0 (event did not occur) and the time to

Published OnlineFirst May 11, 2010; DOI: 10.1158/1078-0432.CCR-09-3199

event (in days) was determined. When an individual was ranked as 0 (event did not occur), a time to event of 88 days (number of days in the 12.5-week study) was recorded. χ^2 and P values were determined by the Log-rank test, using the GraphPad Prism software. A P value of <0.05 was considered significant.

Results

In vitro *cytotoxicity of PLD compared with IL-PLD.* We previously reported that IL-PLD bound to a CD22-expressing cell line (Raji) but did not bind to Jurkat cells (a CD22-negative T-leukemia cell line; ref. 19). Our previous *in vitro* data also showed that IL-PLD exhibited greater cytotoxicity and a lower IC_{50} than PLD in CD22-expressing cell lines, whereas in a CD22-negative cell line, IL-PLD exhibited no difference in cytotoxicity or IC_{50} compared with PLD (19). Our current *in vitro* cytotoxicity experiments (Fig. 1) confirm our previous results. IL-PLD treatment of Raji and Ramos cells (both CD22-expressing Burkitt's B-NHL cell lines) induce greater cytotoxicity than corresponding doses of PLD (Fig. 1A and B), whereas IL-PLD offers no improvement over PLD in CD22-negative Jurkat cells (Fig. 1C). Raji cells were used for all further *in vivo* experiments in this study.

Plasma, tumor, and tissue distribution of DXR. Twenty-one days after Raji NHL implantation, Raji xenograft–bearing nude mice were treated i.v. with IL-PLD, PLD, and nonliposomal (NL)-DXR (10 mg DXR/kg). The total DXR concentration in plasma after administration of IL-PLD, PLD, and NL-DXR are shown in Fig. 2A. The DXR concentration in plasma dropped significantly by 1 hour in NL-DXR– treated mice, whereas DXR concentrations for IL-PLD and PLD treatments do not begin to drop substantially until ~8 hours after treatment (Fig. 2A). DXR blood concentrations were slightly higher in the PLD group compared with the IL-PLD group, but both IL-PLD– and PLD-treated mice had a much slower DXR blood clearance than did mice treated with NL-DXR (Fig. 2A). Myelotoxicity was also assessed 24 hours after IL-PLD, PLD, or NL-DXR treatment. Compared with control mice, IL-PLD and PLD treatments resulted in ~2.2-fold lower bone marrow cell counts, whereas NL-DXR treatment resulted in a 4-fold reduction in bone marrow cell counts (Fig. 2B). There was no difference in bone marrow cell counts between IL-PLD and PLD treatments.

Xenograft-bearing mice treated with either IL-PLD or PLD were assessed for differences in biodistribution. Twenty-four hours after treatment, tissues were harvested and the sum total DXR was extracted and measured. Figure 2C shows that there was a 1.8-fold increase in tumor DXR accumulation in IL-PLD– compared with PLD-treated mice. The spleen also showed more DXR accumulation with IL-PLD treatment compared with PLD treatment (1.6-fold increase). The lung showed 10-fold less DXR accumulation with IL-PLD treatment than with PLD. There was no difference in DXR accumulation between treatments for the liver or kidneys (Fig. 2C).

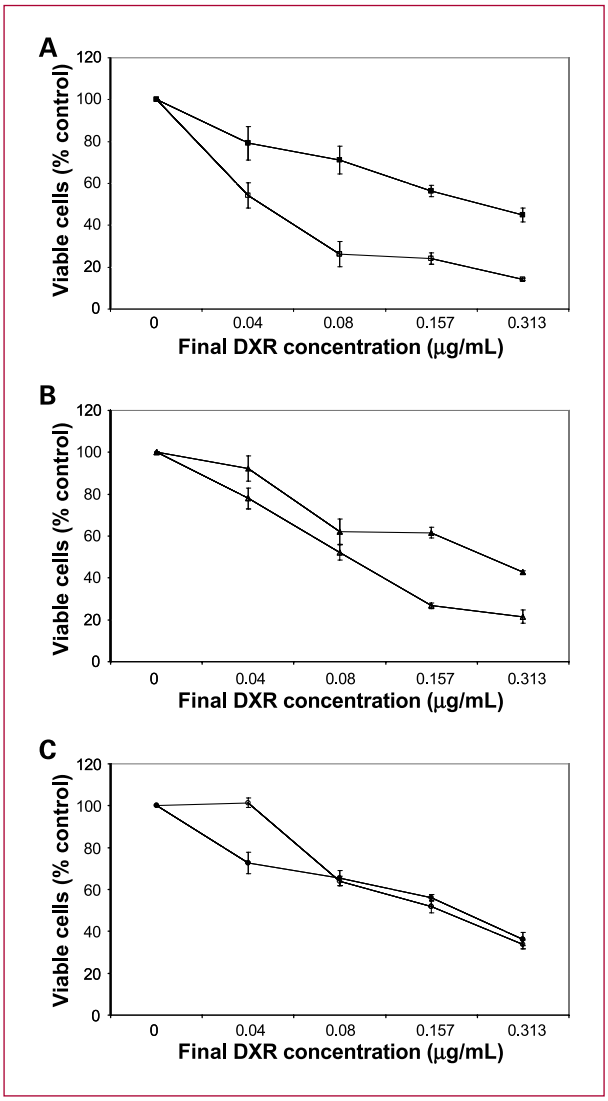

Fig. 1. *In vitro* cytotoxicity of PLD versus IL-PLD in various cell lines. Raji (A), Ramos (B), or Jurkat (C) cells were treated with PLD (filled symbol) or IL-PLD (open symbol) for 72 h, then assessed for viability as described in Materials and Methods. Viability is expressed as % of control (nontreated) cells.

Efficacy and toxicity of IL-PLD. Six groups of xenograft-bearing mice (n = 8 per group) were administered a single dose of PLD or IL-PLD at doses of 8, 12, or 16 mg DXR/kg (Fig. 3A), whereas two additional groups of xenograft-bearing mice (n = 8 per group) received three doses of PLD or IL-PLD at doses of 8 mg/kg/dose on days 1, 8, and 15 (Fig. 3B). At the end of the study, the reduction in tumor volume was greatest in the group treated with three doses of 8 mg DXR/kg IL-PLD (60-fold less than control mice; P = 0.0062; Table 1; Fig. 3A and B). IL-PLD was more effective at reducing tumor volume than was PLD at all dose levels with a 1.8- to 2-fold decrease in tumor volume between corresponding single-dose treatment groups, although the differences between the 12 and 16 mg/kg

Published OnlineFirst May 11, 2010; DOI: 10.1158/1078-0432.CCR-09-3199

groups were not statistically significant (Table 1; Fig. 3A and B). There was a 45-fold decrease in tumor volume between corresponding three-dose treatment groups ($P = 0.0067$; Table 1; Fig. 3B). All treatments reduced tumor volume compared with PBS-treated control mice, although single-dose 8 mg/kg PLD, single-dose 12 mg/kg PLD, and three-dose 8 mg/kg PLD groups were not significantly different than the control group (Table 1). All differences between IL-PLD treatment groups and control were statistically significant ($P \leq 0.0285$; Table 1).

Toxicity of single- or three-dose IL-PLD and PLD was assessed by measuring the effects of treatment on peripheral WBC counts and mouse weights. Within the first 3 weeks of therapy, WBC counts did not differ between any treatment groups (Fig. 3C). By week 6, cell counts were ~2-fold lower compared with control in all single-dose PLD or IL-PLD treatment groups (data not shown) and ~4.8-fold lower compared with control for three-dose PLD and IL-PLD treatment groups (Fig. 3C). There was no difference in WBC counts between corresponding PLD and IL-PLD groups. No difference in animal weights was observed between any of the single-dose treatment groups (data not shown) or three-dose treatment groups (Fig. 3D).

To control for the possibility that the efficacy of IL-PLD was due to HB22.7 either alone or immobilized on the liposome, a subsequent xenograft study compared xenograft-bearing mice that were treated with the previously optimized dose and schedule of IL-PLD and PLD (three doses at 8 mg/kg/dose), and compared with PLD plus unconjugated HB22.7, or IL-null on days 1, 8, and 15 after tumor implantation. From week 9 to the end of the study, the IL-PLD–treated mice had the greatest reduction in tumor volume of any treatment group (Fig. 4A). All comparisons of IL-PLD versus other treatment groups were statistically significant ($P \leq 0.0017$; Table 1). IL-PLD treatment also produced 100% survival at 12 weeks compared with 75% survival for PLD treatment, 65% survival for PLD + unconjugated HB22.7 treatment, 38% survival for IL-null treatment, and 0% survival for PBS control treatment (Fig. 4B).

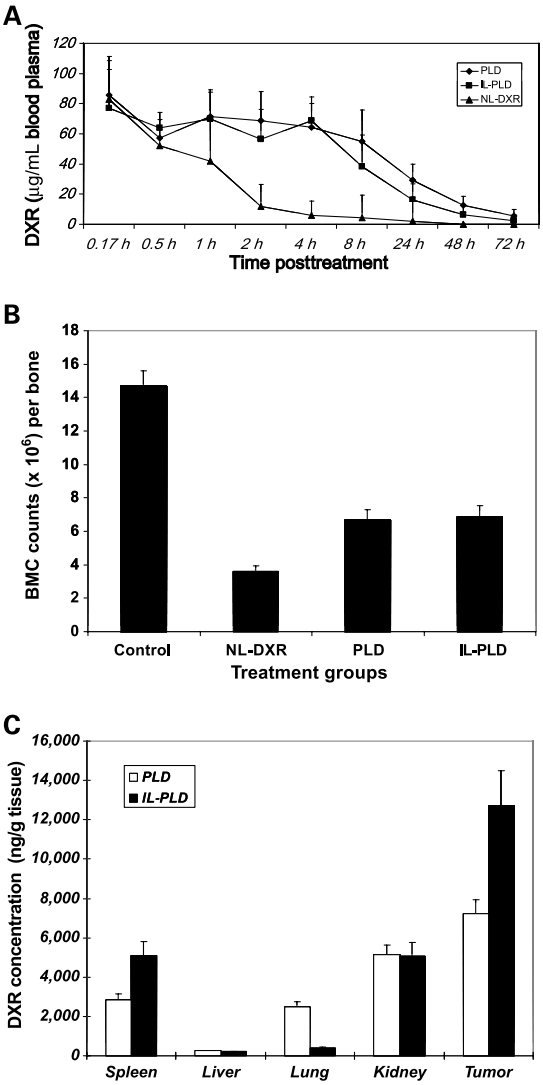

Fig. 2. Plasma DXR clearance, myelotoxicity, and biodistribution of IL-PLD, PLD, and NL-DXR in xenograft-bearing mice. A, blood samples were taken from IL-PLD–treated (■), PLD-treated (♦), and NL-DXR–treated (▲) mice ($n = 4$ per group); blood cells were pelleted; and plasma was collected. DXR was extracted from plasma and quantified. B, mice were treated with 10 mg/kg IL-PLD, PLD, NL-DXR, or PBS ($n = 4$ per group), and 24 hours later, mice were euthanized and bone marrow cells (BMC) were harvested and counted. C, xenograft-bearing mice were treated with 10 mg/kg IL-PLD (filled columns) or PLD (open columns; $n = 4$ per group), and 24 hours later, mice were euthanized and organs were harvested, washed, weighed, and the DXR was extracted and quantified.

Discussion

Liposomal formulations of DXR, such as PLD, offer both increased efficacy and reduced toxicity compared with NL-DXR (7). With the inclusion of mAbs on the liposomal surface, immunoliposomes hold the promise to further reduce toxicity and enhance efficacy compared with nontargeted liposomal therapy. Immunoliposomes designed to bind to a variety of targets (human epidermal growth factor receptor 2, epidermal growth factor receptor, folic acid receptor, B1 integrin, CD19, and CD20) have shown improvement over their nontargeted liposome counterparts in a variety of cancers such as breast carcinoma, glioma, nasopharygeal carcinoma, non–small cell lung carcinoma, and NHL (12, 23–31). Immunoliposomes are an attractive way to deliver drug to an intended target. A typical immunoliposome can encapsulate 15,000 to 45,000 drug molecules per liposome and requires 15 to 40 mAb per liposome for delivery, whereas with a directly conjugated drug, only 8 to 12 molecules of drug can be bound per mAb before mAb binding and stability are affected (32). However, before these immunoliposome products can reach the clinic, there are hurdles that must

Published OnlineFirst May 11, 2010; DOI: 10.1158/1078-0432.CCR-09-3199

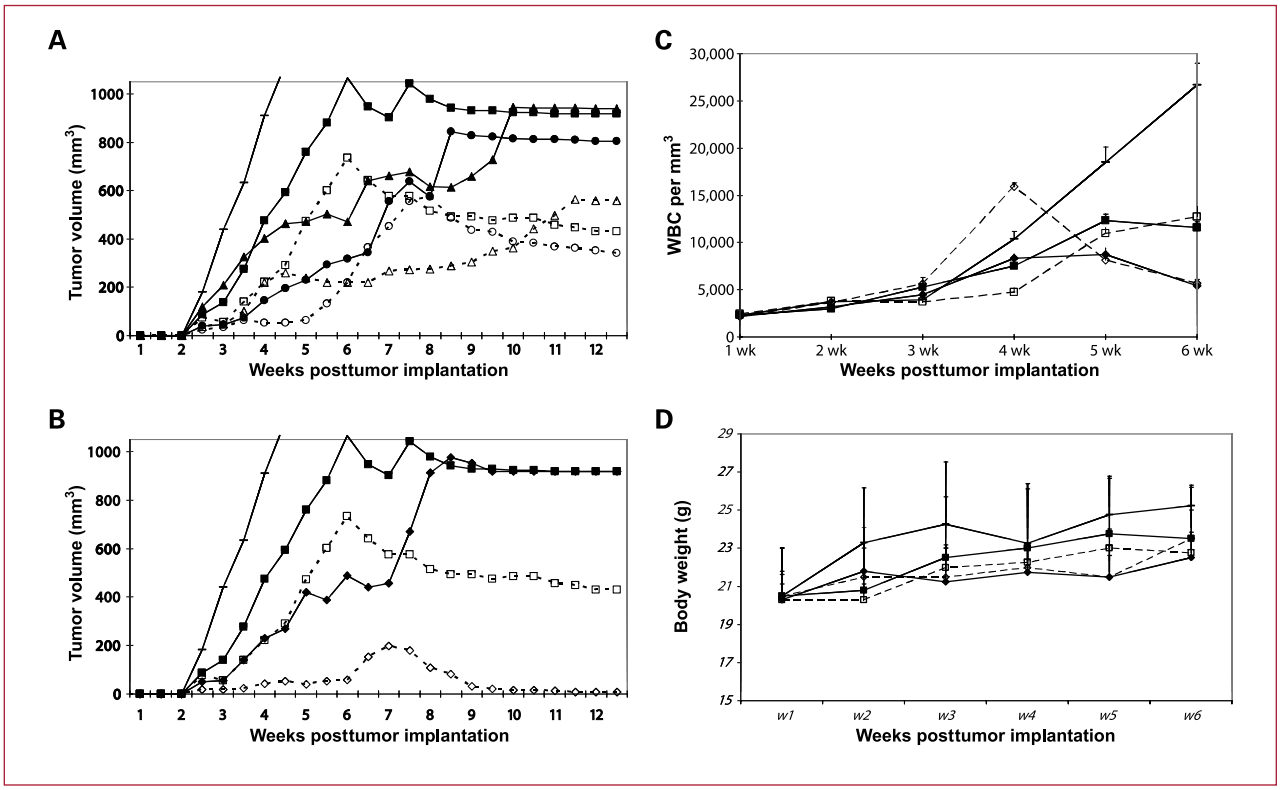

Fig. 3. IL-PLD treatment produced a greater reduction of tumor volume than did PLD with comparable toxicity. Mice were treated with either a single dose of 8 mg/kg (■), 12 mg/kg (▲), or 16 mg/kg (●) or were treated with three doses of 8 mg/kg (♦) PLD (solid line) or IL-PLD (dashed line; $n = 8$ per group). Tumor size was assessed twice weekly. All treatment groups were compared with PBS-treated control mice (+). Tumor volumes were compared in mice treated with the various single doses (A) or 8 mg/kg single versus three dose (B). Toxicity assessment included weekly measurements of WBC counts (C) and mice weights (D).

be overcome. Perhaps the greatest hurdle for liposomes is the inability to specifically target particular tumors. This can be due to the lack of expression of tumor-specific surface antigens or could be due to the phenomenon known as cancer "immunoediting", when a cancer cell under selective pressure from the immune system will downregulate or eliminate the antigen being targeted (33). Another obstacle is caused by the reticuloendothelial system. Although current liposome formulations can, for the most part, avoid sequestration and removal by the reticuloendothelial system (34–37), the inclusion of a whole mAb on the liposomal surface may make them vulnerable to sequestration and removal because the Fc portion of IgG can bind Fc receptors on macrophages (38). This increased macrophage uptake of immunoliposomes can be reduced or eliminated by using Fab or scFv fragments, rather than whole IgG. The immunogenicity of the ligand itself must also be examined before immunoliposomes can be used in the clinic. The mAbs used to create immunoliposomes are often murine, which can cause the formation of human anti-murine antibodies, which, in turn, can alter immunoliposome pharmacokinetics and efficacy (39, 40). Our HB22.7 mAb is currently undergoing such humanization for future clinical testing. Another consideration is the ability of the ligand to induce internalization. Other groups have created CD19- and CD20-targeted immunoliposomal forms of PLD using anti-CD19 and anti-CD20 mAbs (11, 12). Anti-CD20 immunoliposomal PLD showed little improvement over PLD, whereas anti-CD19 immunoliposomal PLD showed greater efficacy than PLD *in vivo* (11, 12). CD20 is a noninternalizing epitope, whereas CD19 is an internalizing epitope. Previous studies have shown that internalizing epitopes are necessary for the efficient delivery of liposomal contents into their target cells (31). Besides the ability of HB22.7 to independently mediate apoptosis of CD22-expressing NHL (16), CD22 may be a better target for immunoliposomal therapy than CD19 for other reasons. A recent study showed that immunotoxins targeted to CD22 exhibit greater internalization and cytotoxicity than immunotoxins targeted to CD19, despite there being fewer CD22 binding sites per cell than CD19 binding sites (41). CD22 is an ideal target for mAb-mediated drug delivery based on its high expression on most NHL and its ability to mediate internalization after ligand binding (18).

HB22.7-conjugated PLD was developed using postinsertion technology, creating a CD22-targeted immunoliposomal form of PLD (IL-PLD). This postinsertion technique is relatively rapid and simple, and can achieve >80%

Published OnlineFirst May 11, 2010; DOI: 10.1158/1078-0432.CCR-09-3199

efficiency of micelle-ligand insertion into preformed liposomes under the correct conditions (21, 32). In our previous study, we determined that IL-PLD remained stable and exhibited equivalent free drug leakage as PLD and is only slightly larger than PLD (165 versus 118 nm mean diameter; ref. 19). Inclusion of HB22.7 onto the surface of PLD was expected to further enhance efficacy and decrease toxicity by targeting PLD to CD22-expressing NHL.

This study is the first to evaluate the plasma pharmacokinetics, biodistribution, and efficacy of CD22-targeted IL-PLD *in vivo*. The plasma pharmacokinetics of DXR in IL-PLD-treated mice was compared with PLD- and NL-DXR–treated mice. Although initial concentrations of plasma DXR are the same for all treatment groups at the earliest time point, the clearance of NL-DXR from the plasma is very rapid (Fig. 2A), whereas DXR clearance after IL-PLD and PLD treatments is much slower and had equivalent clearance rates.

Table 1. χ^2 and *P* values for xenograft studies

PLD vs IL-PLD dose-response study (Fig. 3)	**χ^2**	***P***
Ctrl vs 8 mg/kg PLD single dose	0.1454	0.7029
Ctrl vs 12 mg/kg PLD single dose	2.496	0.1141
Ctrl vs 16 mg/kg PLD single dose	**7.504**	**0.0062**
Ctrl vs 8 mg/kg 3 doses	3.646	0.0562
Ctrl vs 8 mg/kg IL-PLD single dose	**4.795**	**0.0285**
Ctrl vs 12 mg/kg IL-PLD single dose	**4.922**	**0.0265**
Ctrl vs 16 mg/kg IL-PLD single dose	**7.504**	**0.0062**
Ctrl vs 8 mg/kg IL-PLD 3 doses	**7.504**	**0.0062**
PLD vs 8 mg/kg IL-PLD single dose	**6.8**	**0.0091**
PLD vs 12 mg/kg IL-PLD single dose	0.7242	0.3948
PLD vs 16 mg/kg IL-PLD single dose	0.02425	0.8762
PLD vs 8 mg/kg IL-PLD 3 doses	**7.344**	**0.0067**
8 mg/kg PLD single dose vs 8 mg/kg PLD 3 doses	**4.795**	**0.0285**
8 mg/kg IL-PLD single dose vs 8 mg/kg IL-PLD 3 doses	**4.268**	**0.0388**
PLD vs IL-PLD vs IL-null study (Fig. 4)	**χ^2**	***P***
Ctrl vs PLD	**20.5**	**<0.0001**
Ctrl vs IL-PLD	**26.5**	**<0.0001**
Ctrl vs PLD + free HB22.7	**10.79**	**0.001**
Ctrl vs IL-null	**11.48**	**0.0007**
IL-PLD vs PLD	**12.94**	**0.0003**
IL-PLD vs PLD + free HB22.7	**14.87**	**0.0001**
IL-PLD vs IL-null	**9.824**	**0.0017**
PLD vs PLD + free HB22.7	0.3052	0.5806
PLD vs IL-null	0.08097	0.776
IL-null vs PLD + free HB22.7	0.1559	0.693

NOTE: Data were analyzed using the modified Kaplan-Meier curves and the Log-rank test as described in Materials and Methods. Comparisons with significant *P* values (<0.05) are shown in bold.
Abbreviation: Ctrl, control.

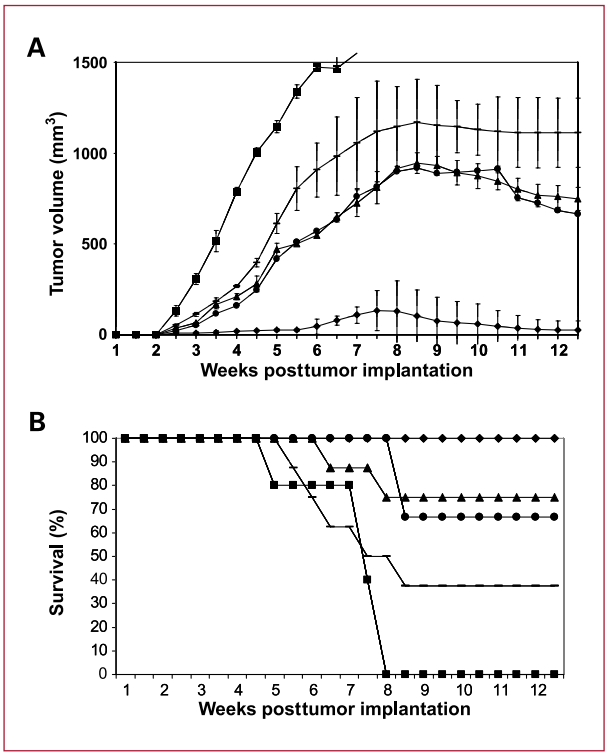

Fig. 4. IL-PLD produced more reduction in tumor volume and enhanced survival versus PLD- or HB22.7-conjugated empty liposomes (IL-null). Mice were treated with IL-PLD (♦), PLD (▲), PLD plus unconjugated HB22.7 (●), or IL-null (+) on day 1, 8, and 15 after tumor implantation ($n = 8$ per group). All groups were compared with PBS-treated control (■). A, tumor volume. B, survival.

IL-PLD and PLD had similar effects on the bone marrow with an approximate 2.2-fold reduction of bone marrow cell counts compared with control mice (Fig. 2B), but the magnitude of the reduction is less than what was observed in the NL-DXR treatment group (4-fold reduction versus control mice). This indicates that IL-PLD and PLD are less myelotoxic than NL-DXR and that IL-PLD is no more myelotoxic than unmodified PLD.

Comparison of the biodistribution of PLD versus IL-PLD at 24 hours posttreatment shows that the greatest DXR accumulation occurs in the tumor and that accumulation is 1.8-fold greater for IL-PLD compared with PLD-treated mice (Fig. 2C) and is consistent with our previous *in vitro* study (19). The spleen showed a 1.6-fold increase in DXR accumulation with IL-PLD treatment compared with PLD treatment (Fig. 2C). Because HB22.7 does not target mouse CD22, this increased splenic uptake is likely due to HB22.7 Fc–mediated binding within the reticuloendothelial system of the spleen. However, despite this increased splenic uptake, there was no increased toxicity in the IL-PLD–treated mice and the T/NT ratio of DXR

Published OnlineFirst May 11, 2010; DOI: 10.1158/1078-0432.CCR-09-3199

accumulation was similar between IL-PLD and PLD treatments (2.5 and 2.3, respectively). The lungs of IL-PLD–treated mice showed 10-fold less DXR accumulation and a much higher T/NT ratio (50 versus 2.8) than the lungs of PLD-treated mice (Fig. 2C). There was no difference in DXR accumulation between treatment groups for the liver or kidneys (Fig. 2C); however, the liver T/NT ratio was greater for IL-PLD–treated mice than for PLD-treated mice (62.5 versus 35).

Our previous study showed that IL-PLD exhibited greater cytotoxicity (3.1- to 5.4-fold decrease in IC_{50}) versus PLD in CD22-expressing cell lines, whereas IL-PLD and PLD cytotoxicity was the same in CD22-negative cell lines (19). Our current *in vitro* cytotoxicity experiments confirm these previous results (Fig. 1). Given these *in vitro* results and given that IL-PLD treatment results in enhanced DXR accumulation in tumors compared with PLD, it was hypothesized than IL-PLD would show enhanced therapeutic efficacy compared with PLD. We assessed the efficacy of three different single-dose treatments of PLD and IL-PLD (8, 12, and 16 mg/kg DXR; Fig. 3A). The differences between the control group and the PLD groups only reached statistical significance for the 16 mg/kg single-dose PLD (Table 1). In comparison, the differences between the control group and the IL-PLD groups were significant for every dosage group (Table 1). Each single-dose IL-PLD treatment group (8, 12, or 16 mg/kg) had 1.8- to 2-fold greater reduction in tumor volume when compared with the corresponding dose of PLD, although the differences between the 12 and 16 mg/kg groups were not statistically different (Table 1; Fig. 3A). In an attempt to improve efficacy without increasing toxicity, a multidose regimen was assessed and compared. A single dose of PLD or IL-PLD (8 mg/kg) was compared with three weekly treatments at the same dose. A highly significant reduction in tumor volume was seen in the group treated with three doses of 8 mg/kg IL-PLD: 45-fold greater reduction in tumor volume when compared with PLD ($P = 0.0067$) and 60-fold reduction when compared with control mice ($P = 0.0062$; Table 1; Fig. 3B).

Previous studies have shown that lipid immobilization of antibodies can improve preclinical efficacy. Thus, to assess both the effects of HB22.7 immobilization and the potentially additive effects of unconjugated HB22.7 in combination with PLD, we compared the efficacy of PLD and IL-PLD to empty liposomes conjugated with HB22.7 (IL-null) and PLD plus nonconjugated HB22.7. PLD or IL-PLD was administered at 8.0 mg DXR/kg/dose. At this dose of IL-PLD, the corresponding lipid and HB22.7 mAb doses were 0.8 to 1 μmol of phospholipids and 200 μg HB22.7 per dose. As described in Materials and Methods, all treatments were administered such that each group received equivalent amounts of phospholipids (1 μmol per dose) or HB22.7 (200 μg per dose). Although IL-null–treated mice had a considerable reduction in tumor volume when compared with controls, again the greatest reduction in tumor volume was in mice treated with IL-PLD (Fig. 4A). This confirms that the efficacy of IL-PLD was not only due to the additive effects of free HB22.7 plus PLD or due to the immobilization of HB22.7 to the surface of liposomes. It is interesting that IL-null–treated mice experienced a considerable reduction in tumor volume when compared with controls, at a fraction of the HB22.7 dose used in previous studies. This is hypothesized to be due to the effects of HB22.7 immobilization. However, this effect alone cannot explain the enhanced efficacy of IL-PLD over PLD. Additionally, when using survival as an end point, IL-PLD was clearly superior when compared with all other treatment groups with 100% survival 12 weeks after treatment initiation (Fig. 4B).

In terms of toxicity, there was no difference in WBC between PLD and IL-PLD treatment groups for the first 3 weeks of treatment (Fig. 3C). As expected, by week 6, WBC counts were ~2-fold lower for PLD and IL-PLD single-dose treatment groups when compared with control (data not shown); however, there were no differences seen between corresponding dosage-specific PLD and IL-PLD treatments. In the mice treated with three doses of PLD or IL-PLD, there was a 4.8-fold reduction in WBC count by week 6 for both PLD and IL-PLD when compared with nontreated controls, but again no differences were seen between corresponding PLD and IL-PLD treatments (Fig. 3C). In addition, there was no significant difference in animal weights among all treatment groups (Fig. 3D). When assessing the toxicity of IL-PLD in terms of peripheral WBC counts, bone marrow cellularity, and animal weights, there is no significant difference when compared with PLD.

In conclusion, IL-PLD showed a significantly greater reduction in human NHL xenograft tumor volume and superior survival when compared with PLD, without increased toxicity. IL-PLD has similar plasma pharmacokinetics compared with PLD and the improvement in efficacy is likely due to improved T/NT ratios and greater DXR tumor delivery. These results indicate that CD22-targeted IL-PLD has distinct advantages over standard PLD and may become a promising new therapeutic for CD22-positive NHL that can be rapidly translated into the clinic given the availability of PLD and humanized HB22.7.

Disclosure of Potential Conflicts of Interest

No potential conflicts of interest were disclosed.

Grant Support

Veterans Administration Merit Award, Leukemia and Lymphoma Society Translational Research Award, The Schwedler Family Foundation, and The deLeuze Endowment for the Nontoxic Cure of Lymphoma.

The costs of publication of this article were defrayed in part by the payment of page charges. This article must therefore be hereby marked *advertisement* in accordance with 18 U.S.C. Section 1734 solely to indicate this fact.

Received 01/06/2010; revised 03/16/2010; accepted 03/28/2010; published OnlineFirst 05/11/2010.

Published OnlineFirst May 11, 2010; DOI: 10.1158/1078-0432.CCR-09-3199

References

1. Ries L, Melbert D, Krapcho M, et al. SEER Cancer Statistics Review, 1975-2005. Bethesda (MD): National Cancer Institute; 2008.
2. Schumer ST, Joyce RM. Radioimmunotherapy for non-Hodgkin's lymphoma. Progress in Oncology 2003:46–72.
3. Hortobagyi GN. Anthracyclines in the treatment of cancer. An overview. Drugs 1997;54 Suppl 4:1–7.
4. Legha SS, Benjamin RS, Mackay B, et al. Reduction of doxorubicin cardiotoxicity by prolonged continuous intravenous infusion. Ann Intern Med 1982;96:133–9.
5. Gralla EJ, Fleischman RW, Luthra YK, et al. The dosing schedule dependent toxicities of adriamycin in beagle dogs and rhesus monkeys. Toxicology 1979;13:263–73.
6. Henderson BM, Dougherty WJ, James VC, et al. Safety assessment of a new anticancer compound, mitoxantrone, in beagle dogs: comparison with doxorubicin. I. Clinical observations. Cancer Treat Rep 1982;66:1139–43.
7. Northfelt DW, Martin FJ, Working P, et al. Doxorubicin encapsulated in liposomes containing surface-bound polyethylene glycol: pharmacokinetics, tumor localization, and safety in patients with AIDS-related Kaposi's sarcoma. J Clin Pharmacol 1996;36:55–63.
8. Maeda H, Sawa T, Konno T. Mechanism of tumor-targeted delivery of macromolecular drugs, including the EPR effect in solid tumor and clinical overview of the prototype polymeric drug SMANCS. J Control Release 2001;74:47–61.
9. Gabizon A, Martin F. Polyethylene glycol-coated (pegylated) liposomal doxorubicin. Rationale for use in solid tumours. Drugs 1997;54 Suppl 4:15–21.
10. Symon Z, Peyser A, Tzemach D, et al. Selective delivery of doxorubicin to patients with breast carcinoma metastases by stealth liposomes. Cancer 1999;86:72–8.
11. Allen TM, Mumbengegwi DR, Charrois GJ. Anti-CD19-targeted liposomal doxorubicin improves the therapeutic efficacy in murine B-cell lymphoma and ameliorates the toxicity of liposomes with varying drug release rates. Clin Cancer Res 2005;11:3567–73.
12. Sapra P, Allen TM. Improved outcome when B-cell lymphoma is treated with combinations of immunoliposomal anticancer drugs targeted to both the CD19 and CD20 epitopes. Clin Cancer Res 2004;10:2530–7.
13. Tedder TF, Tuscano J, Sato S, et al. CD22, a B lymphocyte-specific adhesion molecule that regulates antigen receptor signaling. Annu Rev Immunol 1997;15:481–504.
14. Sato S, Tuscano JM, Inaoki M, et al. CD22 negatively and positively regulates signal transduction through the B lymphocyte antigen receptor. Semin Immunol 1998;10:287–97.
15. Tuscano JM, Riva A, Toscano SN, et al. CD22 cross-linking generates B-cell antigen receptor-independent signals that activate the JNK/SAPK signaling cascade. Blood 1999;94:1382–92.
16. Tuscano JM, O'Donnell RT, Miers LA, et al. Anti-CD22 ligand-blocking antibody HB22.7 has independent lymphomacidal properties and augments the efficacy of 90Y-DOTA-peptide-Lym-1 in lymphoma xenografts. Blood 2003;101:3641–7.
17. Tuscano J, Engel P, Tedder TF, et al. Engagement of the adhesion receptor CD22 triggers a potent stimulatory signal for B cells and blocking CD22/CD22L interactions impairs T-cell proliferation. Blood 1996;87:4723–30.
18. Haas KM, Sen S, Sanford IG, et al. CD22 ligand binding regulates normal and malignant B lymphocyte survival *in vivo*. J Immunol 2006;177:3063–73.
19. O'Donnell RT, Martin SM, Ma Y, et al. Development and characterization of CD22-targeted pegylated-liposomal doxorubicin (IL-PLD). Invest New Drugs 2009.
20. Sakakibara T, Chen FA, Kida H, et al. Doxorubicin encapsulated in sterically stabilized liposomes is superior to free drug or drug-containing conventional liposomes at suppressing growth and metastases of human lung tumor xenografts. Cancer Res 1996;56:3743–6.
21. Ishida T, Iden DL, Allen TM. A combinatorial approach to producing sterically stabilized (Stealth) immunoliposomal drugs. FEBS Lett 1999;460:129–33.
22. Fiske C, Subbarow Y. The colorimetric determination of phosphorus. J Biol Chem 1925;66:375–400.
23. Park JW, Hong K, Carter P, et al. Development of anti-p185HER2 immunoliposomes for cancer therapy. Proc Natl Acad Sci U S A 1995;92:1327–31.
24. Park JW, Hong K, Kirpotin DB, et al. Anti-HER2 immunoliposomes: enhanced efficacy attributable to targeted delivery. Clin Cancer Res 2002;8:1172–81.
25. Ahmad I, Longenecker M, Samuel J, et al. Antibody-targeted delivery of doxorubicin entrapped in sterically stabilized liposomes can eradicate lung cancer in mice. Cancer Res 1993;53:1484–8.
26. Sugano M, Egilmez NK, Yokota SJ, et al. Antibody targeting of doxorubicin-loaded liposomes suppresses the growth and metastatic spread of established human lung tumor xenografts in severe combined immunodeficient mice. Cancer Res 2000;60:6942–9.
27. Lee RJ, Low PS. Folate-mediated tumor cell targeting of liposome-entrapped doxorubicin *in vitro*. Biochim Biophys Acta 1995;1233:134–44.
28. Gabizon A, Horowitz AT, Goren D, et al. Targeting folate receptor with folate linked to extremities of poly(ethylene glycol)-grafted liposomes: *in vitro* studies. Bioconjug Chem 1999;10:289–98.
29. Mamot C, Drummond DC, Greiser U, et al. Epidermal growth factor receptor (EGFR)-targeted immunoliposomes mediate specific and efficient drug delivery to EGFR- and EGFRvIII-overexpressing tumor cells. Cancer Res 2003;63:3154–61.
30. Lopes de Menezes DE, Pilarski LM, Allen TM. *In vitro* and *in vivo* targeting of immunoliposomal doxorubicin to human B-cell lymphoma. Cancer Res 1998;58:3320–30.
31. Sapra P, Allen TM. Internalizing antibodies are necessary for improved therapeutic efficacy of antibody-targeted liposomal drugs. Cancer Res 2002;62:7190–4.
32. Noble CO, Kirpotin DB, Hayes ME, et al. Development of ligand-targeted liposomes for cancer therapy. Expert Opin Ther Targets 2004;8:335–53.
33. Dunn GP, Bruce AT, Ikeda H, et al. Cancer immunoediting: from immunosurveillance to tumor escape. Nat Immunol 2002;3:991–8.
34. Allen TM, Hansen C. Pharmacokinetics of stealth versus conventional liposomes: effect of dose. Biochim Biophys Acta 1991;1068:133–41.
35. Allen TM, Hansen C, Martin F, et al. Liposomes containing synthetic lipid derivatives of poly(ethylene glycol) show prolonged circulation half-lives *in vivo*. Biochim Biophys Acta 1991;1066:29–36.
36. Gabizon A, Catane R, Uziely B, et al. Prolonged circulation time and enhanced accumulation in malignant exudates of doxorubicin encapsulated in polyethylene-glycol coated liposomes. Cancer Res 1994;54:987–92.
37. Senior J, Delgado C, Fisher D, et al. Influence of surface hydrophilicity of liposomes on their interaction with plasma protein and clearance from the circulation: studies with poly(ethylene glycol)-coated vesicles. Biochim Biophys Acta 1991;1062:77–82.
38. Joshi T, Butchar JP, Tridandapani S. Fcγ receptor signaling in phagocytes. Int J Hematol 2006;84:210–6.
39. Klee GG. Human anti-mouse antibodies. Arch Pathol Lab Med 2000; 124:921–3.
40. Van Kroonenburgh MJ, Pauwels EK. Human immunological response to mouse monoclonal antibodies in the treatment or diagnosis of malignant diseases. Nucl Med Commun 1988;9:919–30.
41. Du X, Beers R, Fitzgerald DJ, et al. Differential cellular internalization of anti-CD19 and -CD22 immunotoxins results in different cytotoxic activity. Cancer Res 2008;68:6300–5.

AACR American Association for Cancer Research

Clinical Cancer Research

Efficacy, Biodistribution, and Pharmacokinetics of CD22-Targeted Pegylated Liposomal Doxorubicin in a B-cell Non–Hodgkin's Lymphoma Xenograft Mouse Model

Joseph M. Tuscano, Shiloh M. Martin, Yunpeng Ma, et al.

Clin Cancer Res 2010;16:2760-2768. Published OnlineFirst May 11, 2010.